Supplement of Atmos. Chem. Phys., 20, 15443–15459, 2020
https://doi.org/10.5194/acp-20-15443-2020-supplement

Atmospheric Chemistry and Physics
Open Access
EGU

Supplement of

Airborne measurements of fire emission factors for African biomass burning sampled during the MOYA campaign

Patrick A. Barker et al.

Correspondence to: Patrick A. Barker (patrick.barker@manchester.ac.uk)

Supplementary material

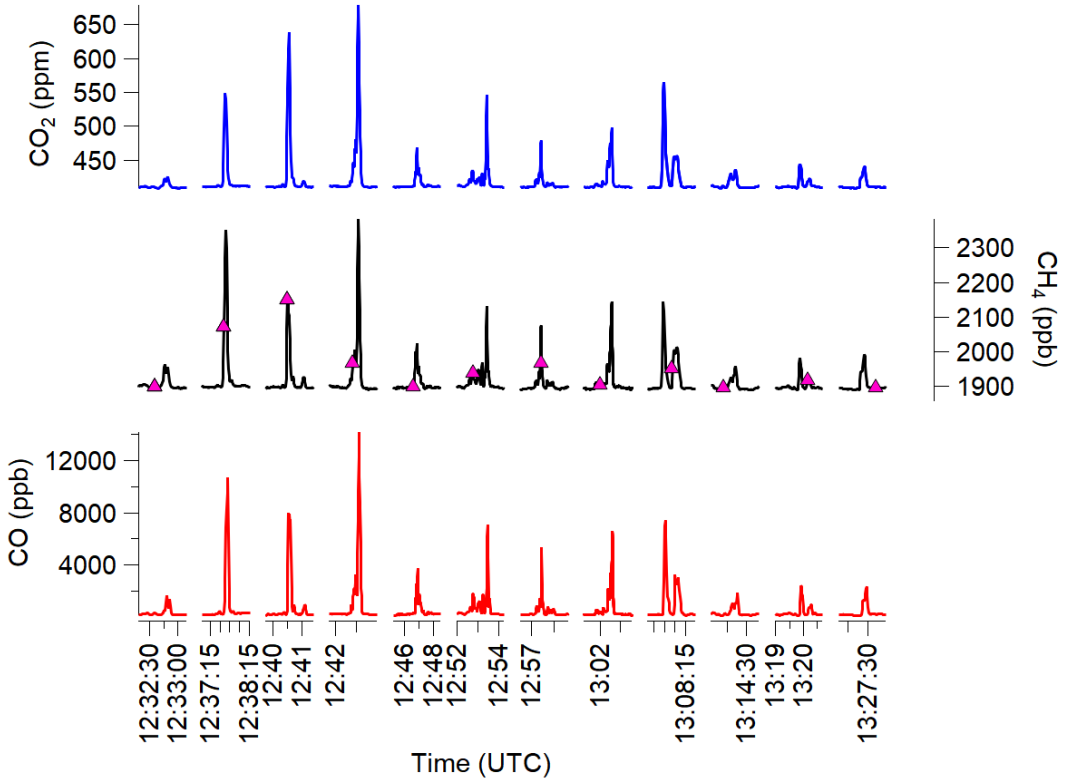

Figure S1: time series of CO (red), CH_4 (black), CO_2 (blue) and concentrations in the plumes analysed for flight C005. Median WAS canister fill times are marked on the CH_4 time series as pink triangles. Note that some WAS taken in background regions are not shown here.

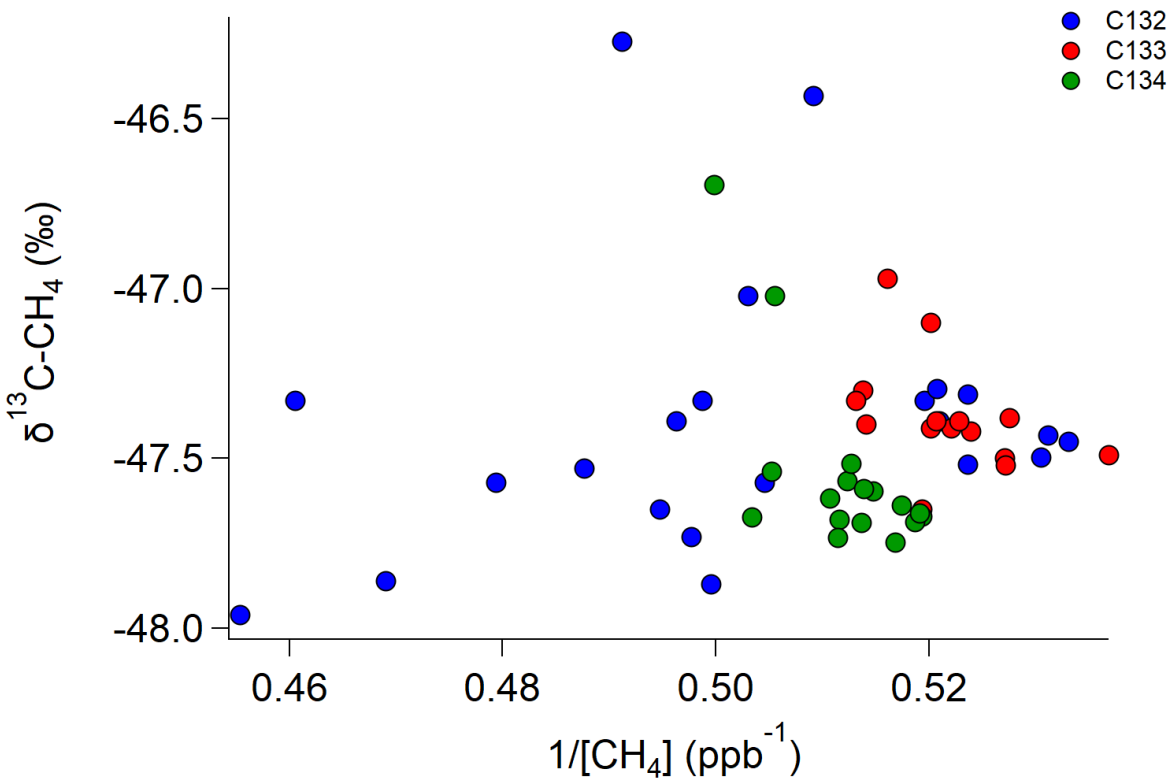

Figure S2: Keeling plot (δ^{13}C-CH_4 vs inverse CH_4 mixing ratio) for all isotope samples taken during the MOYA-II (Uganda) flights C132 (blue), C133 (red) and C134 (green).

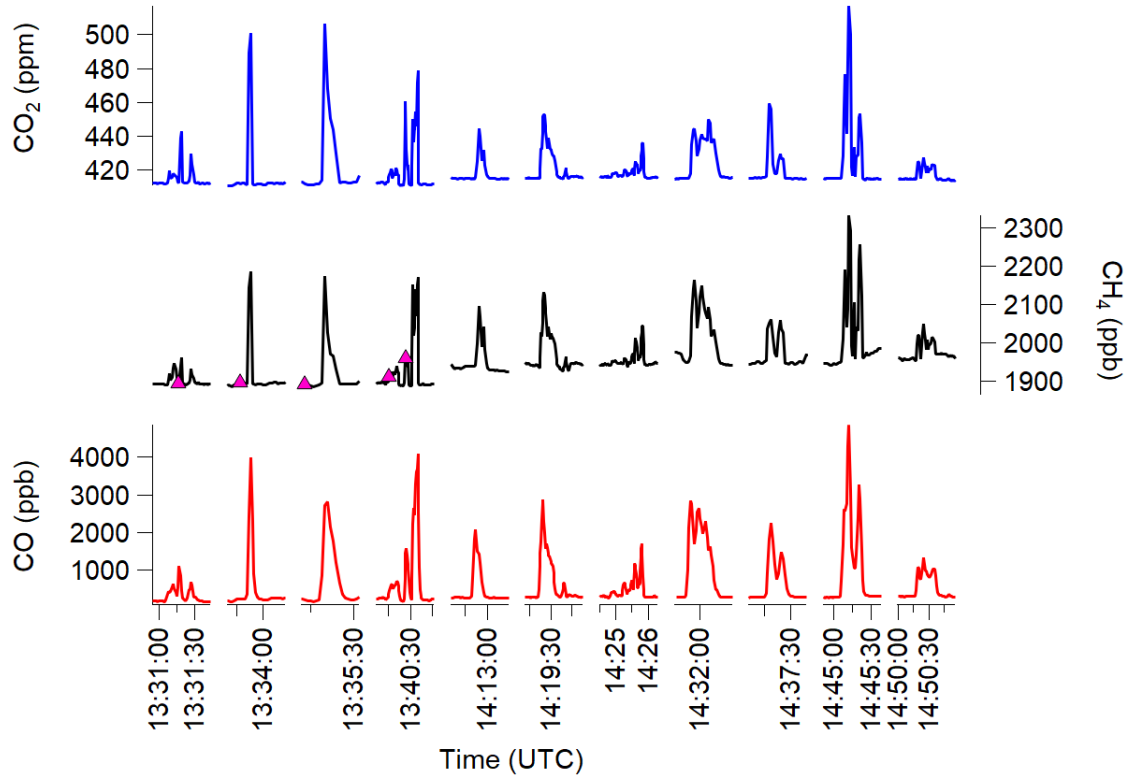

Figure S3: time series of CO (red), CH_4 (black), CO_2 (blue) and concentrations in the plumes analysed for flight C133. Median WAS canister fill times are marked on the CH_4 time series as pink triangles. Note that some WAS taken in background regions are not shown here.

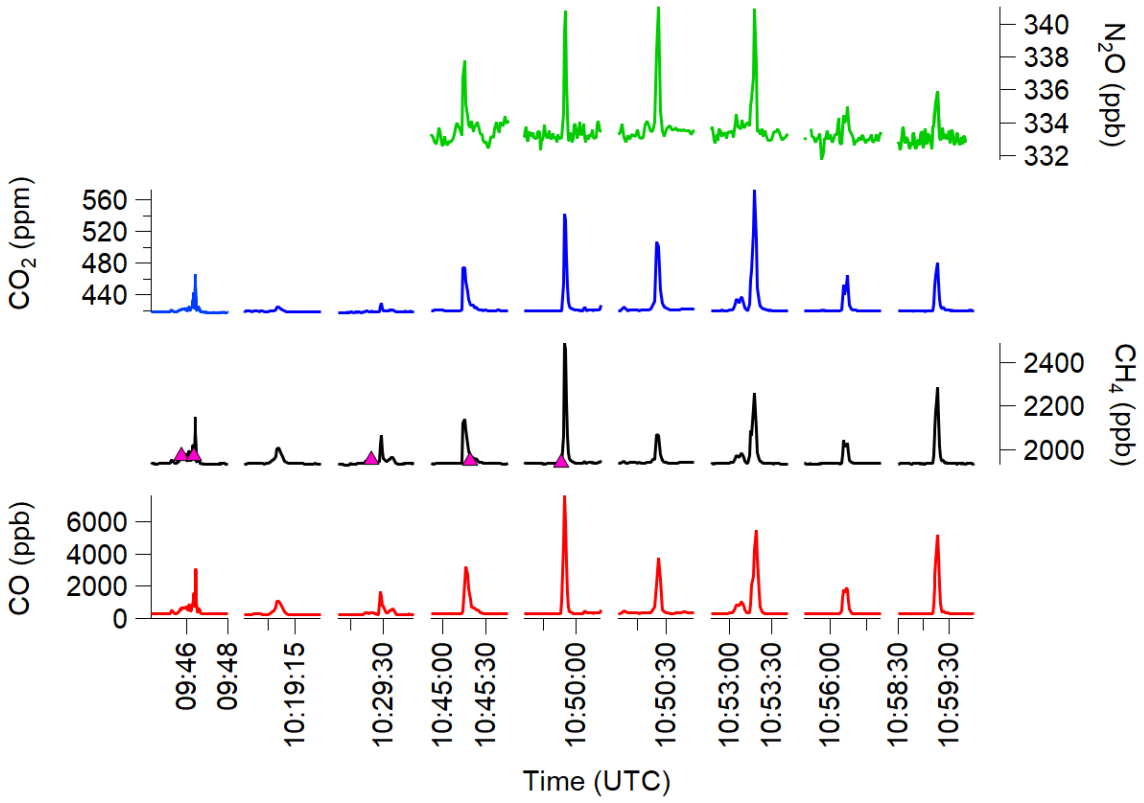

Figure S4: time series of CO (red), CH_4 (black), CO_2 (blue) and N_2O (green) concentrations in the nine plumes analysed for flight C134. N_2O data quality was insufficient for calculation of EF for the first three plumes, hence these are not shown. Median WAS canister fill times are marked on the CH_4 time series as pink triangles. Note that some WAS taken in background regions are not shown here.

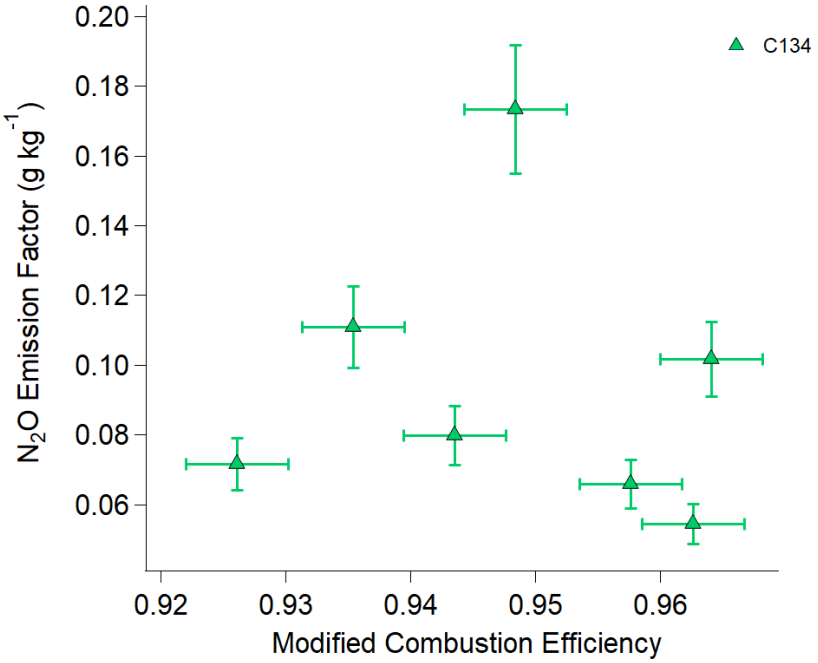

Figure S5: N_2O EF vs modified combustion efficiency for six biomass burning plumes sampled in flight C134 during MOYA-II.

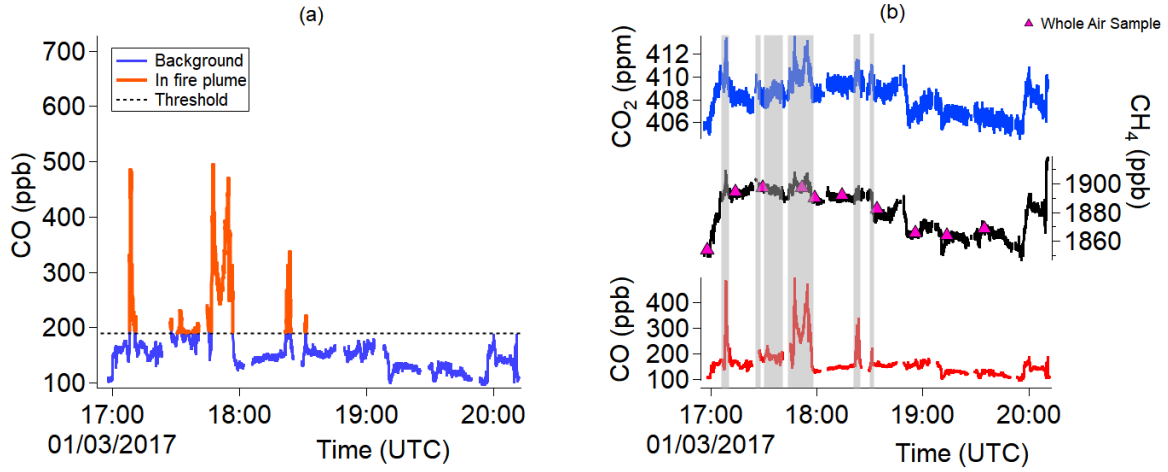

Figure S6: (a) CO mixing ratio time series over the course of flight C006, with the plumes exceeding the statistical threshold shown in orange and the background shown in purple. The plume selection threshold is also shown as a dashed line. (b) time series of CO (red), CH_4 (black) and CO_2 (blue) concentrations over flight C006, the biomass burning plumes chosen for analysis are highlighted in grey. Median WAS canister collection times are shown as pink triangles

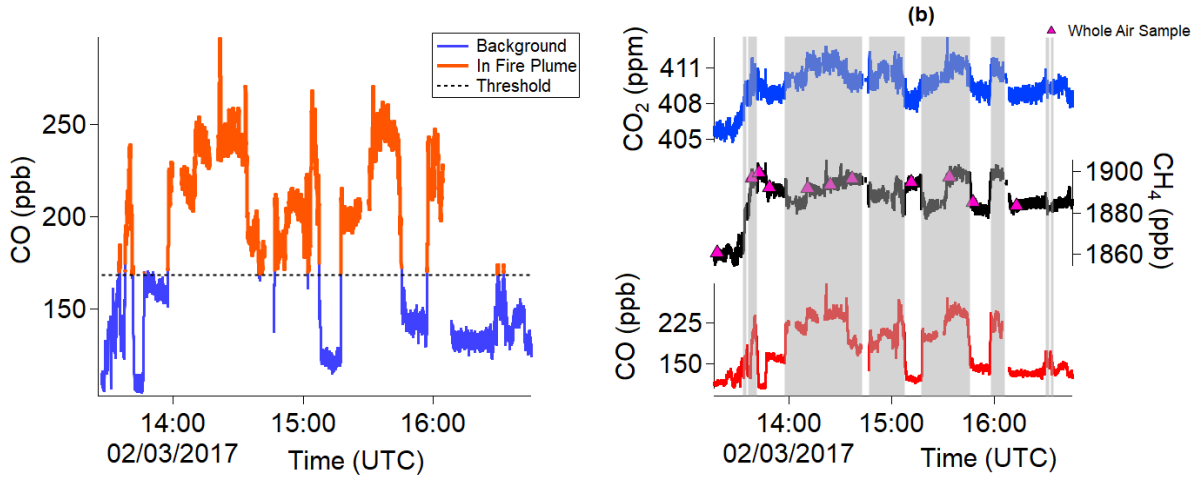

Figure S7: (a) CO mixing ratio time series over the course of flight C006, with the plumes exceeding the statistical threshold shown in orange and the background shown in purple. The plume selection threshold is also shown as a dashed line. (b) time series of CO (red), CH_4 (black) and CO_2 (blue) concentrations over flight C006, the biomass burning plumes chosen for analysis are highlighted in grey. Median WAS canister collection times are shown as pink triangles

Comparison of peak integration and regression method for emission factor calculation

During this work, two separate methods were used to calculate emission ratios (ER). The first method involves using the integrated plume area with background subtracted in the concentration time series for each plume, the second uses weighted regression analysis of in-plume species vs in-plume tracer CO from which ER with respect to CO is obtained from the gradient. Both analytical methods have been used to calculate ERs and emission factors (EF) for both the near-field and far-field fire emissions. The comparison between the two methods is presented here.

The regression analyses of the near-field flights are shown in Fig. S8 and S9. For the MOYA-II near-field flights where HCN was used as a biomass burning tracer, A seven standard deviation CO threshold above mean background was used to select in-plume data as is used for the MOYA-I near-field flights. For the integration analysis of the far-field flights, all enhanced in-plume data (Fig. S6 and S7) is treated as a single 'plume', and the averaged background subtracted from the integrated area under all in-plume data is used to calculate one ER per flight. The CH_4 and CO_2 EFs and their respective uncertainties calculated from each method are shown in Fig. S10.

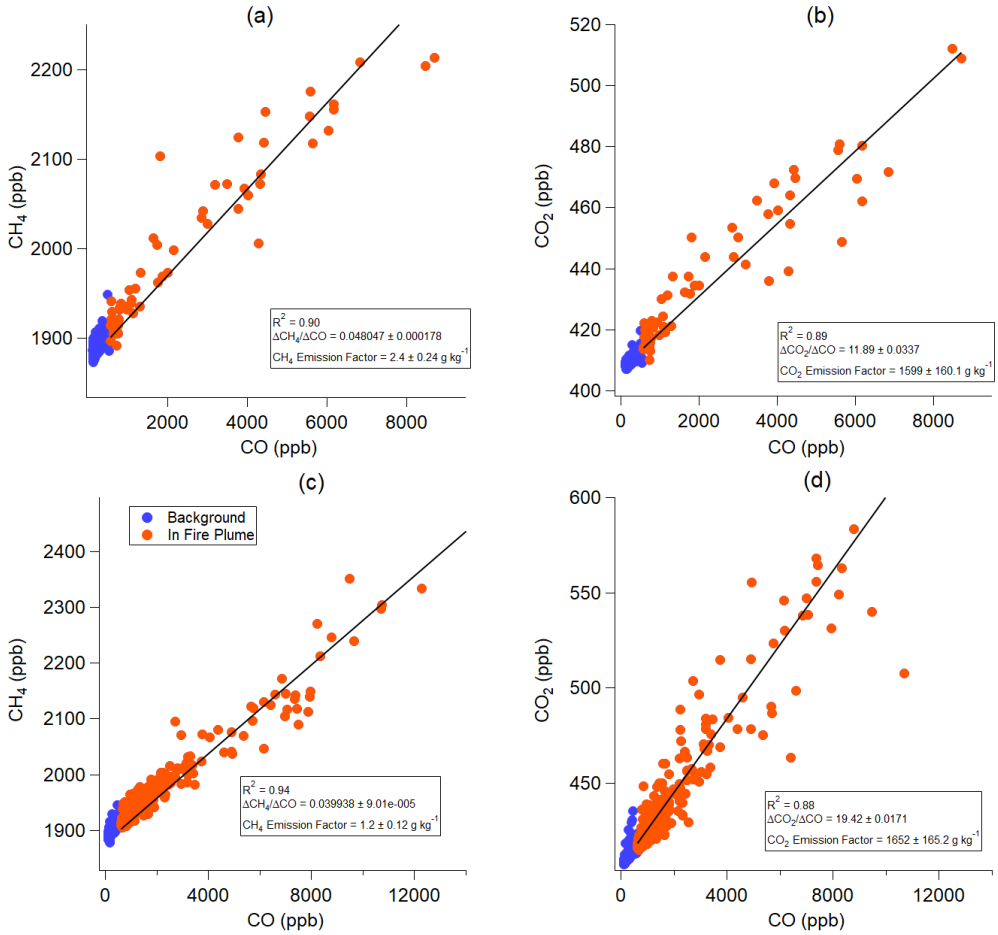

Figure S8: Linear regressions of in-plume (a) CH_4 and (b) CO_2 mixing ratio versus in-plume CO mixing ratio for flight C004 and (c) CH_4 and (d) CO_2 mixing ratio versus in-plume CO for flight C005. The linear regressions are calculated using the York regression method, and are weighted towards CO and CH_4/CO_2 measurement uncertainty (York et al. 2004). ERs obtained from the slope are also shown, as well as the calculated EFs.

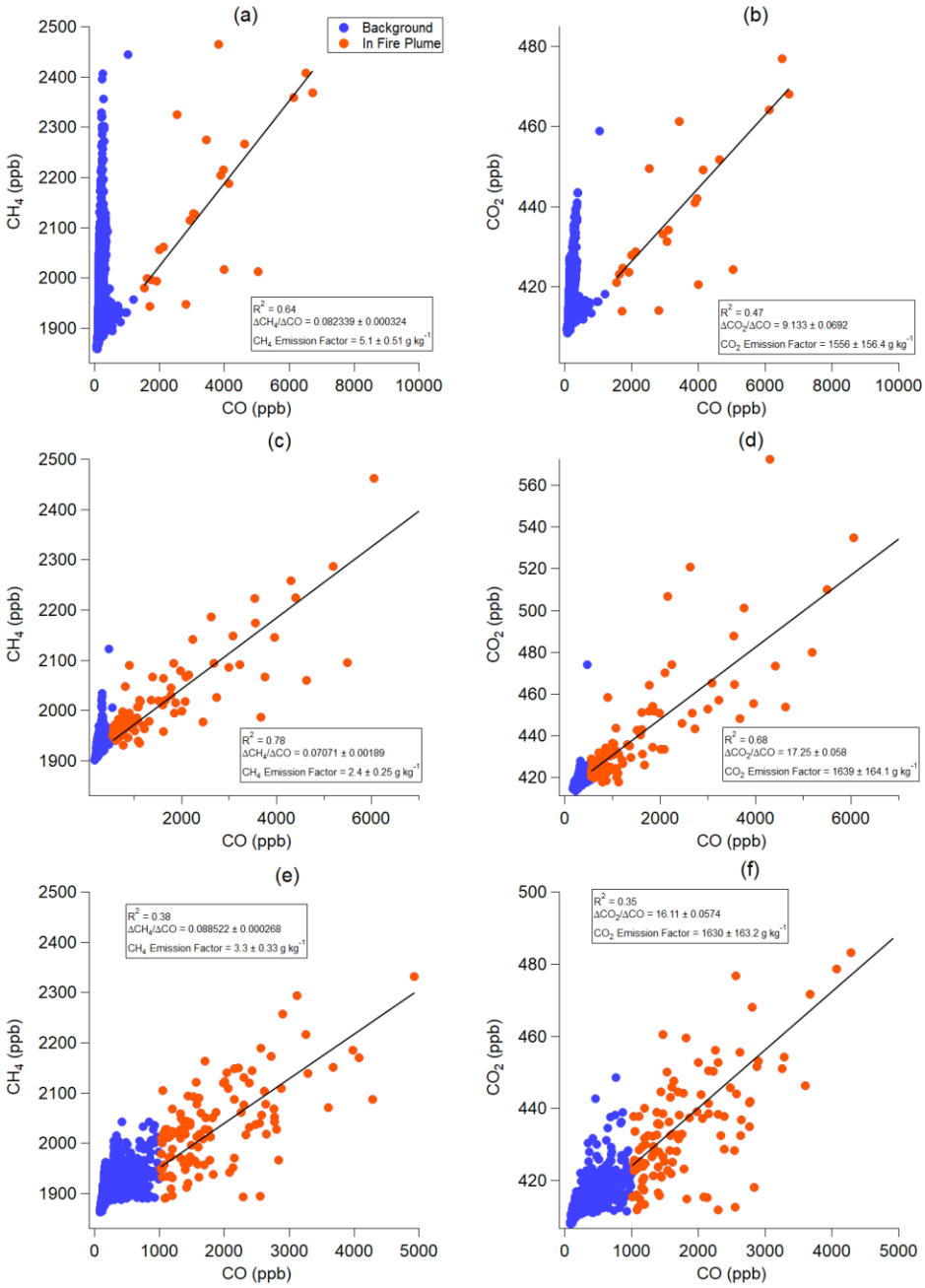

Figure S9: Linear regressions of in-plume (a) CH_4 and (b) CO_2 mixing ratio versus in-plume CO mixing ratio for flight C132 (c) CH_4 and (d) CO_2 versus in-plume CO for flight C133 and (e) CH_4 and (4) CO_2 versus in-plume CO for flight C134. The linear regressions are calculated using the York regression method, and are weighted towards CO and CH_4/CO_2 measurement uncertainty (York et al. 2004). ERs obtained from the slope are also shown, as well as the calculated EFs.

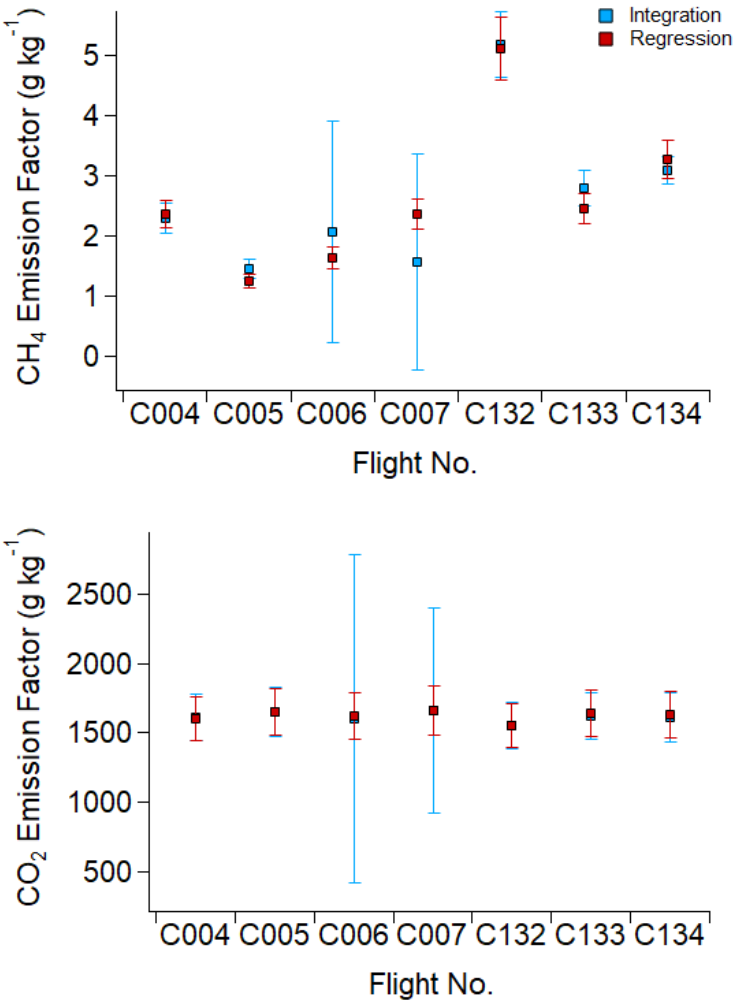

Figure S10: Comparison of CH_4 and CO_2 EFs and their respective uncertainties calculated using the integration method (blue) and regression analysis (red).

It can be seen from Fig. S10 that there is good agreement between the two methods of calculating ER for both CO2 and CH_4. The uncertainties of C006 and C007 integration EF are notably larger than uncertainties for all other EF, this is due to the high variability in the background in the far-field flights and relatively small enhancement over the background in the plume compared to the near-field flights.

For the near-field flights C004, C005, C132, C133 and C134, the integration method is chosen as this allows calculation of specific EFs for each fire plume, whereas the regression analysis only yields one EF per flight in this case. Regression analysis is chosen for the far-field flights as the EF yielded from this method have a significantly smaller uncertainty than those determined via the integration method.